8-1-2019

An In Vitro Enrichment Strategy for Formulating Synergistic Synbiotics

Car Reen Kok

David Fabian Gomez Quintero

Clement Niyirora

Devin Rose

Amanda Li

See next page for additional authors

Authors

Car Reen Kok, David Fabian Gomez Quintero, Clement Niyirora, Devin Rose, Amanda Li, and Robert Hutkins

AMERICAN SOCIETY FOR MICROBIOLOGY | Applied and Environmental Microbiology®

MICROBIAL ECOLOGY

An *In Vitro* Enrichment Strategy for Formulating Synergistic Synbiotics

Car Reen Kok,[a] David Fabian Gomez Quintero,[a] Clement Niyirora,[a] Devin Rose,[a] Amanda Li,[a]* Robert Hutkins[a]

[a]Department of Food Science and Technology, Nebraska Food for Health Center, Lincoln, Nebraska, USA

ABSTRACT Research on the role of diet on gut and systemic health has led to considerable interest toward identifying novel therapeutic modulators of the gut microbiome, including the use of prebiotics and probiotics. However, various host responses have often been reported among many clinical trials. This is in part due to competitive exclusion as a result of the absence of ecological niches as well as host-mediated constraints via colonization resistance. In this research, we developed a novel *in vitro* enrichment (IVE) method for isolating autochthonous strains that can function as synergistic synbiotics and overcome these constraints. The method relied on stepwise *in vitro* fecal fermentations to enrich for and isolate *Bifidobacterium* strains that ferment the prebiotic xylooligosaccharide (XOS). We subsequently isolated *Bifidobacterium longum* subsp. *longum* CR15 and then tested its establishment in 20 unique fecal samples with or without XOS. The strain was established in up to 18 samples but only in the presence of XOS. Our findings revealed that the IVE method is suitable for isolating potential synergistic probiotic strains that possess the genetic and biochemical ability to ferment specific prebiotic substrates. The IVE method can be used as an initial high-throughput screen for probiotic selection and isolation prior to further characterization and *in vivo* tests.

IMPORTANCE This study describes an *in vitro* enrichment method to formulate synergistic synbiotics that have potential for establishing autochthonous strains across multiple individuals. The rationale for this approach—that the chance of survival of a bacterial strain is improved by providing it with its required resources—is based on classic ecological theory. From these experiments, a human-derived strain, *Bifidobacterium longum* subsp. *longum* CR15, was identified as a xylooligosaccharide (XOS) fermenter in fecal environments and displayed synergistic effects *in vitro*. The high rate of strain establishment observed in this study provides a basis for using synergistic synbiotics to overcome the responder/nonresponder phenomenon that occurs frequently in clinical trials with probiotic and prebiotic interventions. In addition, this approach can be applied in other protocols that require enrichment of specific bacterial populations prior to strain isolation.

KEYWORDS bifidobacteria, prebiotic, probiotic, synbiotic, xylooligosaccharide

It is now well accepted that the composition and function of the gastrointestinal microbiome play a major role in maintaining host health (1, 2). How the human gut microbiome is affected by diet is one of the most important areas of research in the food, nutrition, and biomedical sciences (3, 4). In particular, a disrupted or dysbiotic microbiota has been suggested to contribute to a wide range of gastrointestinal and systemic diseases (5). Researchers are now especially interested in developing therapeutic or dietary approaches to correct or redress these imbalances (6, 7).

A frequent outcome of many biomedical reports and clinical trials is the observation that a particular treatment may be effective in some individuals but not in others (8–11). This responder/nonresponder phenomenon is also common in trials

Citation Kok CR, Gomez Quintero DF, Niyirora C, Rose D, Li A, Hutkins R. 2019. An *in vitro* enrichment strategy for formulating synergistic synbiotics. Appl Environ Microbiol 85:e01073-19. https://doi.org/10.1128/AEM.01073-19.

Editor Edward G. Dudley, The Pennsylvania State University

Address correspondence to Robert Hutkins, rhutkins1@unl.edu.

* Present address: Amanda Li, University of Texas Health Science Center at Houston, Houston, Texas, USA.

Received 9 May 2019
Accepted 6 June 2019
Accepted manuscript posted online 14 June 2019
Published 1 August 2019

using probiotics, prebiotics, and other gut health interventions (12, 13). For example, while prebiotic supplementations have been shown in numerous clinical studies to induce a bifidogenic response (14–16), there are often study participants for whom this expected response does not occur (13, 17, 18). Identifying or predicting responders and nonresponders based on their resident microbiota remains a significant challenge (13).

Several explanations may account for the nonresponder phenotype. For prebiotics, nonresponders may lack the relevant strains that are physiologically or biochemically equipped to utilize that particular substrate. Alternatively, even if such strains were present, other members of the microbiota may simply outcompete those strains for the substrate. Similarly, probiotics are also subject to host-specific effects. To reach the colon, it is possible that ingested strains may not survive digestion through the stomach and small intestine (19). In the colon, they may be inhibited or outcompeted by other gut commensals.

One approach to enrich for beneficial microbes in the gut is to introduce specific strains in the form of synbiotics. Ideally, these synbiotics would be composed of prebiotic-probiotic combinations, such that the prebiotic is specifically and preferentially fermented by the probiotic. The rationale for this approach is based on classic ecological theory. Specifically, Tilman's resource ratio competition model states that the dominance of certain taxa is dependent upon the availability and demand for particular resources along with the rate of nutrient consumption (20, 21). Thus, if the synbiotic was formulated such that the prebiotic specifically stimulated the growth of the companion probiotic, the latter would have a greater opportunity to become established in the gut. Indeed, previous studies described the possible persistence of probiotics when administered as a synbiotic (22, 23).

Synbiotics that are appropriately designed also have the potential to increase the responder rate, by converting nonresponders into responders (12). These so-called synergistic synbiotics were envisioned more than a decade ago (24), but few successful formulations of synergistic synbiotics have been reported (25). This is most likely due to the lack of strategic methods for pairing prebiotics and probiotics that can demonstrate synergism.

Recently, we described one such approach called *in vivo* selection, or IVS (25). Briefly, an autochthonous strain of *Bifidobacterium adolescentis* was enriched *in vivo* by the prebiotic galactooligosaccharide (GOS) and then recovered by cultural methods (13, 26). When the enriched strain (*B. adolescentis* IVS-1) was recombined with GOS as a synbiotic and introduced to rodents, the abundance of IVS-1 increased to 37%, which was significantly higher than those for the prebiotic- and probiotic-only controls (25). The enhanced abundance of the IVS-1 strain was considered to be due to the ability of this strain to consume GOS more rapidly than its competitors, including other resident bifidobacteria. Although the abundance of IVS-1 was not increased when combined with the prebiotic in human subjects, the strain still reached higher levels of abundance than an allochthonous strain of *Bifidobacterium* (12).

Despite the potential of the IVS approach for isolating autochthonous synergistic strains with putative beneficial properties, this method requires, at minimum, that a human subject study be conducted. In contrast, if a reproducible *in vitro* strategy could be devised to mimic the IVS method, it would be possible to obtain similar strains in a faster and more cost-effective manner.

This study proposes the concept of *in vitro* enrichment (IVE) as an alternative strategy to select for potentially synergistic putative probiotic strains. Autochthonous strains of *Bifidobacterium* were enriched through a stepwise batch fecal fermentation model using a targeted approach. Such strains obtained by IVE would be expected to be competitive in the gut environment when combined with the cognate prebiotic. In this study, we used the prebiotic xylooligosaccharide (XOS) and successfully obtained a *Bifidobacterium* strain that demonstrated synergism when reintroduced with XOS into *in vitro* fecal environments from multiple donors.

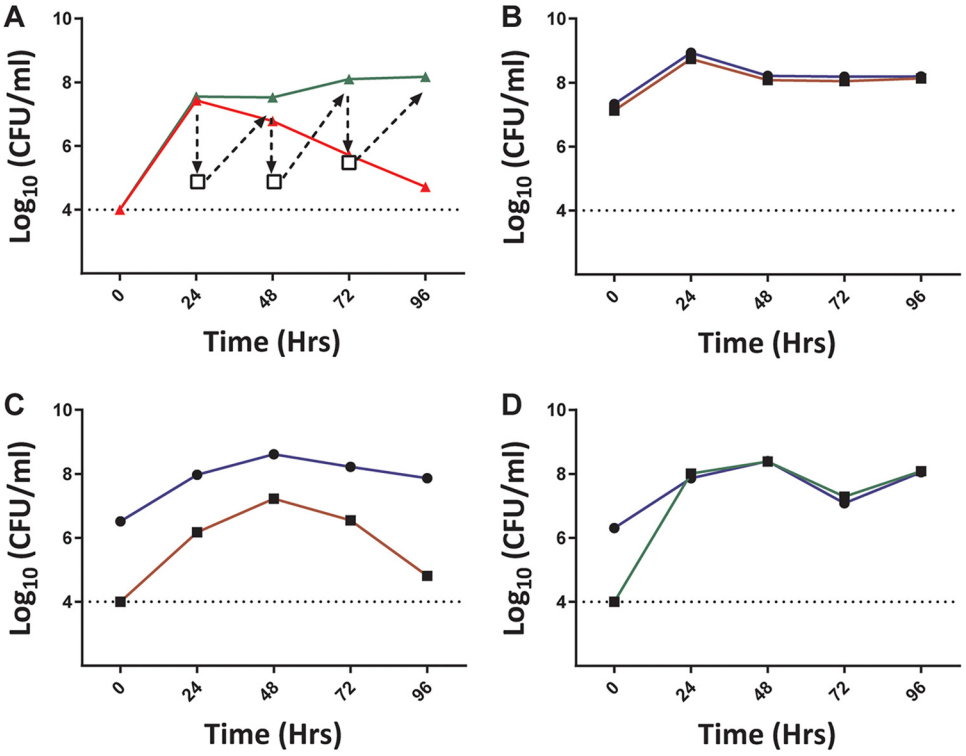

FIG 1 Bifidobacteria were successfully enriched by XOS in fecal environments, whereas strain establishment was dependent on the strain and the host. (A) Hypothetical trends of successful (green) and unsuccessful (red) enrichments in fermentation experiments. (B) Enrichment of total *Bifidobacterium* (●) and *B. adolescentis* (■) in a sample from which *B. adolescentis* CR11 was isolated. (C) Unsuccessful establishment of *B. adolescentis* (CR11) (■) with commensurate enrichment of total *Bifidobacterium* (●) in a sample from which *B. longum* subsp. *longum* CR15 was isolated. (D) Establishment of *B. longum* (CR15) (■) and total *Bifidobacterium* (●). Horizontal dashed lines indicate limits of detection (10^4 CFU/ml).

RESULTS

Enrichment of XOS-utilizing bifidobacterium strains. A total of 60 bifidobacterial isolates were initially obtained from enrichment experiments using 3 different fecal donor samples. A successful enrichment would be predicted by an increase or recovery of specific species of bacteria after every stepwise 100-fold dilution (Fig. 1A). Strains that were not enriched would be expected to be present at low abundance or entirely washed out (below detection levels) at the end of the four fermentation cycles (approximately 25 generations). From the 60 isolates obtained, identification through BLASTn of the 16S rRNA Sanger-based sequences resulted in 7 unique bifidobacterial strains. These included five strains of *B. adolescentis* and one each of *Bifidobacterium pseudocatenulatum* and *Bifidobacterium longum*. Quantification at the genus level using quantitative PCR (qPCR) revealed enrichment of total *Bifidobacterium* in all 3 samples. Specifically, one *B. adolescentis* isolate was obtained from a sample displaying enrichment in species of *B. adolescentis* (Fig. 1B), and this isolate, *B. adolescentis* CR11, was chosen for subsequent establishment experiments.

Establishment of *B. adolescentis* CR11 and discovery of *B. longum* subsp. *longum* CR15. The ability of a strain to become established in an *in vitro* fecal environment was assessed in establishment experiments in a manner similar to that for the XOS enrichment except that the test strain was included along with the prebiotic. A successful establishment was denoted by persistence of the test strain during the test period, whereas a failed establishment was indicated by a decrease in abundance or washout of the test strain over the test period. When *B. adolescentis* CR11 was reintroduced in a new fecal sample along with the prebiotic at the start of fermentation, quantification by genus-specific qPCR revealed that enrichment of *Bifidobacterium* was

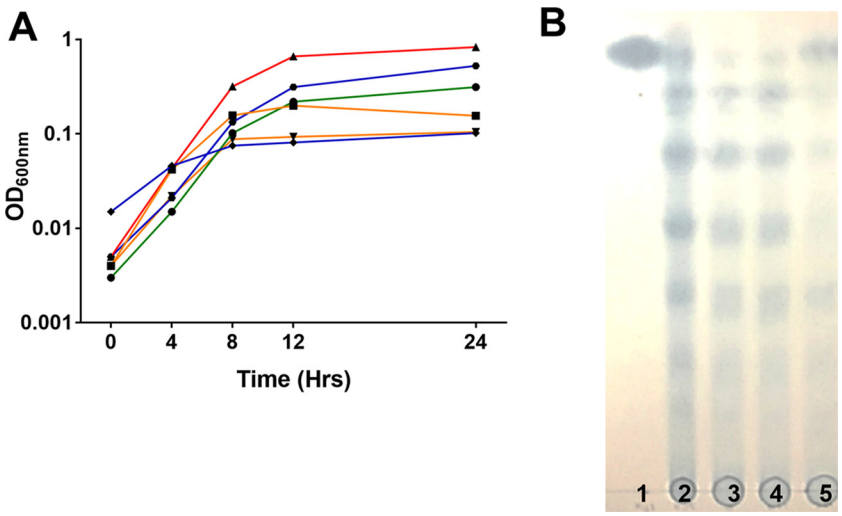

FIG 2 Growth of *B. longum* subsp. *longum* CR15 in minimal media supplemented with different XOS fractions. (A) Optical density measurements at a wavelength of 600 nm every 4 h within the first 12 h and at 24 h using minimal media (◆; mMRS) with the addition of the following sugars: MRS containing equivalent amounts of residual sugars (■; mMRS-res), 1% glucose (▲; mMRS-glucose), 1% XOS (●; mMRS-XOS), 1% of an XOS fraction containing DPs 2, 3, and 4 (⬣; mMRS-DP2,3,4), and 1% of an XOS fraction containing DPs 4 and above (▼; mMRS-DP4). (B) TLC analysis was carried out using 7.5 μl of spent fermentation media and standards including 2.5 μl of 2% xylose and 5 μl of 2% XOS. The plates were developed twice using a solvent containing 1-butanol/2-propanol/H_2O (3:12:4) and sprayed with 0.5% α-naphthol and 5% H_2SO_4 in ethanol. Lane 1, xylose; lane 2, XOS; lane 3, mMRS-XOS; lane 4, 0 h spent medium; lane 5, 24 h spent medium. Growth profiles demonstrated the strain's preference to utilize smaller DPs of XOS.

initially observed (Fig. 1C). However, based on species-specific qPCR, it was evident that *B. adolescentis* had been displaced by other bifidobacteria. Indeed, all of the isolates ($n = 10$) subsequently recovered by culturing were identified as *B. longum* by 16S Sanger sequencing.

The *B. longum* strain (identified as and named *B. longum* subsp. *longum* CR15) was subsequently introduced into another fecal sample. Quantification revealed stable enrichment of *B. longum* species, with 100% of the isolates ($n = 10$) identified as *B. longum* (Fig. 1D). Growth of *B. longum* subsp. *longum* CR15 in modified de Man, Rogosa and Sharpe medium in which glucose was replaced with 1% XOS (mMRS-XOS) and 1% XOS fractions (with degrees of polymerization [DPs] 2 to 4 [mMRS-DP2,3,4] and with DPs 4 and above [mMRS-DP4]) demonstrated that this strain was able to utilize XOS with a preference for polymers with a low degree of polymerization (Fig. 2A and B).

Genome assembly and annotation of *B. longum* subsp. *longum* CR15. Whole-genome sequence data were generated (a total of 296 Mbp), and a draft genome of 2.4 Mbp was assembled with 96% coverage against a reference genome. Annotation against the CAZy database identified several proteins associated with XOS utilization, including the glycosyl hydrolases GH43 and GH120 and carbohydrate binding molecules CBM6 and CBM22. In addition, relevant sugar transport and utilization genes were annotated with Prokka and TransAAP as D-xylulose 5-phosphate (*xfp*), xylose isomerase (*xylA*), xylulokinase (*xylB*), β-xylosidase (*xynB*), xylose import ATP-binding protein (*xylG*), xylose transport system permease protein (*xylH*), and ABC-type xylose transport system (*xylF*). Strain-specific primers targeting the adenine-specific methyltransferase PaeR71 gene were subsequently designed from the genome.

Establishment of *B. longum* subsp. *longum* CR15 is host microbiota dependent. Additional establishment experiments with *B. longum* subsp. *longum* CR15 and XOS were performed using 20 individual donor samples (Fig. 3A). Experiments in the absence of XOS were conducted in parallel and served as controls. In the presence of XOS, strain-specific qPCR quantification revealed that the CR15 strain was clearly established in 7 samples; another 11 demonstrated intermediate establishment (Fig. 3B).

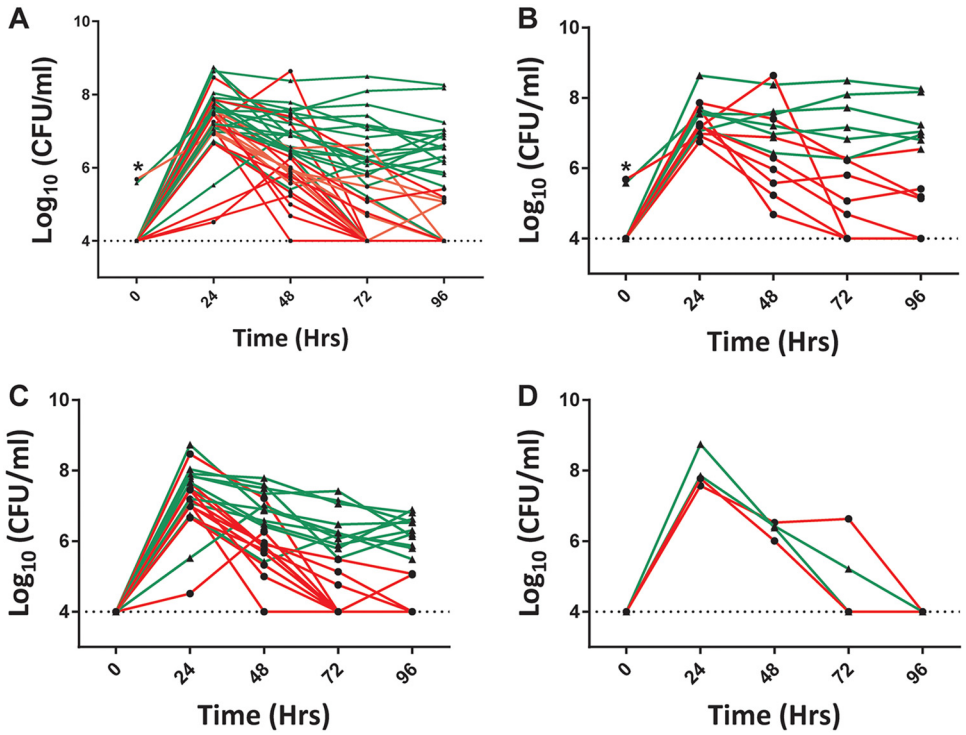

FIG 3 Various trends of establishment of *B. longum* subsp. *longum* CR15 were observed across fecal samples. (A) A summary of the establishment trends of *B. longum* subsp. *longum* CR15 in all 20 samples in the presence (▲) or absence (●) of XOS. *B. longum* subsp. *longum* CR15 was clearly established in 7 samples (B), potentially established in 11 samples (C), and displaced or washed out in 2 samples (D). In the absence of XOS, the strain could not be established in any of the samples. Time zero samples were taken prior to inoculation of 10^7 CFU/ml of the test strains. Horizontal dashed lines indicate the limits of detection (10^4 CFU/ml); * indicates the sample from which *B. longum* subsp. *longum* CR15 was isolated.

The latter included samples in which CR15 levels fluctuated between the start and end of fermentation or decreased by less than 2 log (Fig. 3C). Only in two samples did the CR15 strain fail to become established (Fig. 3D). *B. longum* subsp. *longum* CR15 was either reduced or completely washed out in the no-prebiotic controls. Individual establishment curves emphasize the host-specific response (see Fig. S1 in the supplemental material).

XOS treatment differentially shifts the fecal microbial community. Next, 16S amplicon sequencing was performed to investigate changes in community structure in a subset of 10 samples. This subset of samples was representative of the establishment phenotype observed for all 20 samples and consisted of 4 demonstrating clear establishment of *B. longum* subsp. *longum*, 5 showing intermediate establishment, and 1 failed establishment. To assess alpha diversity of the samples over time, Shannon index and observed amplicon sequence variants (ASVs) were computed. There was an initial significant decrease in diversity (false discovery rate [FDR] < 0.05) from 0 to 24 h for both treatments (Fig. 4A and B). However, no further changes were observed after the first 24-h time point. Throughout the fermentation period, the diversity of the XOS-supplemented samples was significantly lower than that of the no-prebiotic controls (FDR < 0.05). Beta diversity analysis of the samples at baseline and at the end of fermentation was visualized using principal-coordinate analysis (PCoA) based on Bray-Curtis distance. The samples at baseline clustered together, while fermentation samples at 96 h clearly clustered separately based on treatment (Fig. 4C). Principal-component analysis (PCA) revealed that *B. longum*, *Bifidobacterium pseudocatenulatum*, and *Enterococcus faecium* were drivers in the XOS group (Fig. 4D).

Taxonomic analysis of the 16S rRNA sequences revealed a highly bifidogenic response in the presence of XOS as well as significant enrichment of *Lactobacillus* that

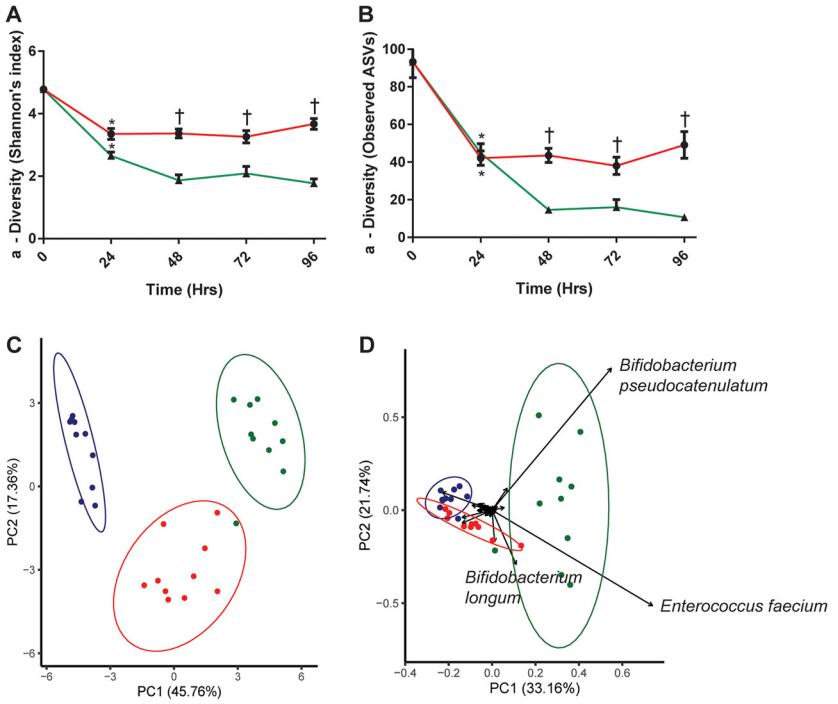

FIG 4 Analysis of microbial community composition and diversity across treatments. By two measures of α-diversity, Shannon index (A) and number of ASVs (B), diversity was lower in the presence of XOS (▲) than in the absence of XOS (●). Principal-coordinate analysis (PCoA) (C) and principal-component analysis (PCA) (D) revealed distinct community profiles between groups at baseline (blue) and at the end of the fermentation period, with (green) or without (red) XOS (PERMANOVA, $P = 0.001$). *, significant difference between 0 and 24 h; †, significant difference between treatments at a particular time point.

was not observed in the no-prebiotic controls (Fig. 5A). Enrichment of *Enterococcus* was also observed after 96 h for both the XOS and no-XOS treatments (Fig. 5A and B). Three specific *Bifidobacterium* ASVs were investigated for their contribution toward the bifidogenic response throughout the fermentation duration (see Fig. S2). BLASTn of

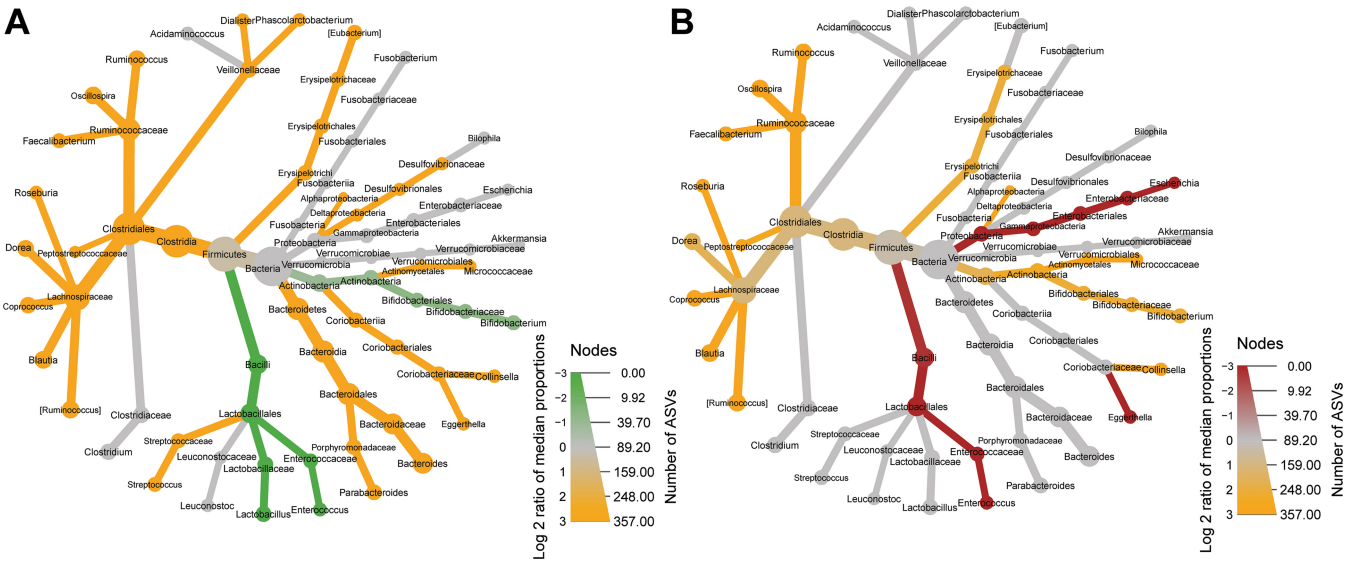

FIG 5 Significant changes in taxa driven by XOS in establishment experiments with *B. longum* subsp. *longum* CR15. Wilcoxon rank sum test with FDR adjustment was used to identify significantly different taxa (FDR < 0.05) in the presence (A) and absence (B) of XOS. Nodes in orange indicate greater abundance at baseline than at 96 h, whereas nodes in green and red indicate greater abundance at 96 h than at baseline.

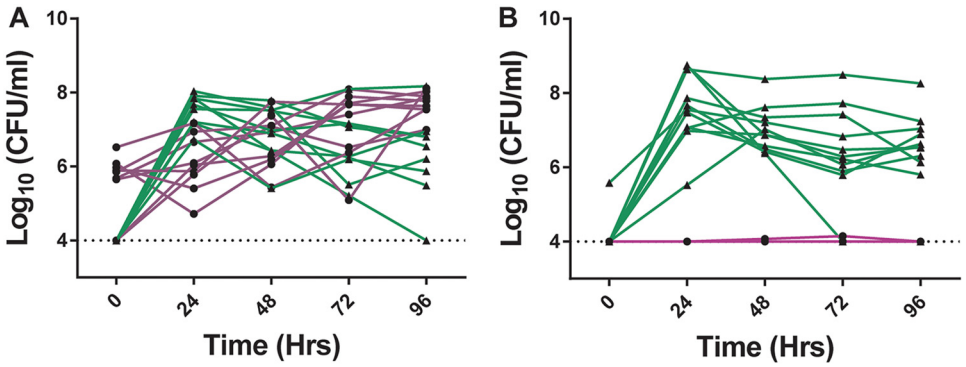

FIG 6 Enrichment of *B. longum* subsp. *longum* CR15 (▲) and *B. pseudocatenulatum* (●) in the presence of XOS. (A) When present at baseline in most samples ($n = 9$), *B. pseudocatenulatum* reached high cell numbers at the end of fermentation. (B) When *B. pseudocatenulatum* was below detection at baseline ($n = 11$), the species remained throughout. Horizontal dashed lines indicate the limits of detection (10^4 CFU/ml).

these specific sequence variants against the NCBI nr database revealed that they belonged to the species *B. longum*, *B. pseudocatenulatum*, and *B. adolescentis*. These species were also previously observed from the 16S Sanger sequencing of isolates that were obtained postfermentation.

Coenrichment of *B. longum* subsp. *longum* CR15 and *B. pseudocatenulatum*. Additional analyses revealed differences in the mean abundances of the *B. longum* and *B. pseudocatenulatum* ASVs between treatments. In the first 24 h, the mean percentage relative abundance of the *B. longum* ASV increased from 4% to 43% in fermentations with XOS but only to 11% in the no-prebiotic controls (Fig. S2A). While a subsequent decrease in abundance of the *B. longum* ASV was observed in both treatments, only 1% remained at 96 h in the controls compared to 10% in the XOS fermentations (Fig. S2A). In addition, there was an average increase from 4% to 29% in the *B. pseudocatenulatum* ASV in the XOS-supplemented fermentations after 96 h (Fig. S2B). Low abundance of the *B. adolescentis* ASV was observed throughout the fermentation in both XOS and no-XOS treatments (Fig. S2C).

The effect of *B. pseudocatenulatum* on persistence of CR15 was determined by species-level qPCR. In most cases ($n = 11$), when *B. pseudocatenulatum* was absent (i.e., below detection) in fecal samples at baseline, levels remained low throughout fermentation, and successful establishment of *B. longum* subsp. *longum* CR15 was observed (Fig. 6B). In contrast, *B. pseudocatenulatum* was able to persist and co-occur with CR15 if detectable levels of this organism were present at baseline ($n = 9$) (Fig. 6A).

To further investigate the persistence potential of *B. longum* subsp. *longum* CR15, a 7-day washout experiment was performed using a subset of 4 of the 20 fecal samples. In 2 samples (subjects 3 and 4), high numbers of *B. longum* subsp. *longum* CR15 were maintained through day 7. However, in the other 2 samples (subjects 14 and 16), *B. longum* subsp. *longum* CR15 was decreased or washed out by day 7, even in the presence of XOS (see Fig. S3A and B). Subsequent 16S amplicon sequencing of these day 7 samples revealed high abundance of two ASVs corresponding to *B. adolescentis* and *B. pseudocatenulatum* (Fig. S3C and D).

Acetate is enriched in XOS-supplemented fermentations. Short and branched-chain fatty acid (S/BCFA) profiles were obtained for all 20 *B. longum* subsp. *longum* CR15 establishment experiments in the presence and absence of XOS. At all time points, acetate levels were highest, followed by lower levels of propionate and butyrate (Table 1). At 24 h, acetate and total SCFA levels were significantly higher in the prebiotic group, whereas by 48 h, butyrate and propionate levels were significantly higher in the control group. By 96 h, the BCFAs isobutyrate and isovalerate were significantly higher in the control group. After 24 h, SCFA production remained generally stable for both treatments.

TABLE 1 Concentrations of S/BCFA from fermentation supernatants of establishment experiments with *B. longum* subsp. *longum* CR15

Microbial metabolite	Mean S/BCFA concn (mM) ± SEM at:								
		24 h		48 h		72 h		96 h	
	0 h	Control	XOS	Control	XOS	Control	XOS	Control	XOS
Acetate	8.72 ± 3.61	18.65 ± 2.35	34.94 ± 3.73[b,a]	11.65 ± 2.18	33.64 ± 3.69[b]	8.94 ± 1.26	41.25 ± 5.03[b]	11.59 ± 1.87	42.24 ± 2.85[b]
Butyrate	0.05 ± 0.01	0.69 ± 0.21[a]	0.53 ± 0.26	1.04 ± 0.21	0.48 ± 0.18[b]	1.07 ± 0.23	0.43 ± 0.21	0.94 ± 0.19	0.35 ± 0.18[b]
Propionate	0.09 ± 0.05	0.5 ± 0.33	0.39 ± 0.19	1.35 ± 0.22[a]	0.06 ± 0.03[b]	1.24 ± 0.23	0.04 ± 0.02[b]	1.46 ± 0.20	0.05 ± 0.02[b]
Total SCFA[c]	8.87 ± 3.64	19.84 ± 2.60[a]	35.85 ± 3.38[b,a]	14.04 ± 2.39	34.18 ± 3.67[b]	11.25 ± 1.61	41.72 ± 5.04[b]	13.99 ± 1.84	42.64 ± 2.85[b]
Isobutyrate	0.01 ± 0.003	0.01 ± 0.004	0.02 ± 0.01	0.07 ± 0.04	0.01 ± 0.01	0.05 ± 0.02	0.003 ± 0.001	0.11 ± 0.05	0.01 ± 0.004[b]
Isovalerate	0.02 ± 0.003	0.02 ± 0.01	0.17 ± 0.12	0.21 ± 0.09	0.18 ± 0.14	0.38 ± 0.18	0.29 ± 0.25[b]	0.19 ± 0.06	0.04 ± 0.02[b]
Total BCFA[d]	0.02 ± 0.005	0.03 ± 0.01	0.18 ± 0.12	0.27 ± 0.11	0.19 ± 0.14	0.43 ± 0.19	0.3 ± 0.25[b]	0.3 ± 0.11	0.05 ± 0.02[b]

[a]Significant difference from the previous time point.
[b]Significant difference between XOS and control treatments within a time point.
[c]SCFA, short-chain fatty acids.
[d]BCFA, branched-chain fatty acids.

PICRUSt was used to assess differences in the abundance of predicted metabolic genes involved in acetate and butyrate production between treatments. Specifically, butyrate kinase, acetate kinase, and acetyl coenzyme A (acetyl-CoA) transferase genes were investigated. As expected, metagenome predictions indicated higher levels of acetate kinase genes in the XOS group. Likewise, higher levels of butyrate kinase and acetyl-CoA transferase genes in the control group were also predicted (Fig. S4). Correlation analysis between genus abundance and S/BCFA concentrations revealed a significant positive correlation between *Bifidobacterium* and *Lactobacillus* with acetate (Fig. S4).

DISCUSSION

In this study, we developed an *in vitro* enrichment (IVE) platform for isolating prebiotic-enriched strains that could be combined with the cognate prebiotic to form synergistic synbiotics. Enrichment was performed using a bifidogenic and highly selective substrate, XOS (27). Overall, 15 unique *Bifidobacterium* isolates were obtained. All belonged to one of three species, *B. adolescentis*, *B. pseudocatenulatum*, and *B. longum*, which are among the predominant resident *Bifidobacterium* species found in adults (28, 29). Of these 3 species, *B. adolescentis* and *B. longum* have been well studied for their probiotic properties as well as for their growth potential on XOS (30–32). In contrast, the probiotic potential of *B. pseudocatenulatum* has not been well explored. However, it is known to ferment dietary fibers, including XOS (33, 34).

Strain establishment is a more complex and challenging process than strain enrichment by prebiotics. Indeed, probiotic microbes rarely persist after the supplementation period has ended (35, 36). This is due, in part, to the individuality and highly competitive nature of the gut microbiome as well as the absence of open ecological niches (37). These factors likely contribute to the responder/nonresponder phenomenon that is commonly observed in dietary intervention studies (13, 38). Thus, the absence of an available ecological or functional niche could inhibit or prevent the establishment of a particular strain (35).

In contrast, provision of a prebiotic or other specialized nutrient, along with a suitable probiotic, could provide a new nutrient niche (39), enhance persistence, and reduce the frequency of nonresponder phenotypes. In this *in vitro* study, combining the XOS-enriched *B. longum* subsp. *longum* CR15 strain with XOS promoted strain establishment in most of the 20 unique fecal samples, with steady-state populations maintained at approximately 10^7 CFU/ml. Although variation in the persistence phenotype was observed, the CR15 strain was unable to persist in only two samples. XOS-dependent establishment was confirmed by the rapid washout of CR15 in fermentations in the absence of the prebiotic.

While qPCR was useful for measuring populations of specific genera, species, or strains, community sequencing provided an independent basis for assessing changes in microbial composition. Taxonomic results confirmed that enrichment of *B. longum*

occurred as a result of XOS supplementation. This observation also suggested that a specific *B. longum* ASV that was present in high abundance was representative of the CR15 strain, although it may be composed of other closely related *B. longum* strains that shared high 16S sequence similarity.

Interestingly, community analysis also revealed that the *B. longum* ASV/CR15 strain was not always the dominant *Bifidobacterium*. In some samples, *B. pseudocatenulatum* and *B. adolescentis*, as represented by two other unique ASVs, were prevalent during the fermentations, and their growth was clearly supported by the presence of XOS. In particular, *B. pseudocatenulatum* was present in high abundance across multiple samples. This was further confirmed by qPCR showing that levels of *B. pseudocatenulatum* remained high during the entire fermentation when present at baseline. Both methods suggested that *B. pseudocatenulatum* was also enriched by XOS. In some samples, an observed relative low abundance/absence of *B. longum* subsp. *longum* when *B. pseudocatenulatum* abundance was high suggested these two microbes were niche competitors.

The synbiotic treatment led to significantly lower alpha diversity measures, likely due to the enrichment of bifidobacteria. This was further confirmed in the PCA plot where *Bifidobacterium* was a major driver differentiating the two treatments. Reduced diversity was previously observed in *in vitro* studies of fiber fermentation (40–43).

When the stepwise fermentations were extended to 7 days, CR15 again persisted in the presence of XOS for the first 4 days. However, beyond day 4, persistence was more variable. When CR15 was washed out, increased populations of *B. adolescentis* and *B. pseudocatenulatum* were observed.

SCFAs are beneficial by-products of gut metabolism that are associated with carbohydrate fermentation (44, 45). Like other SCFAs, acetate serves as an energy source for epithelial cells and comprises a high percentage of the total SCFA produced in the gut (39). In the presence of XOS, the higher concentrations of acetate were likely due to fermentation by *Bifidobacterium*. However, the low butyrate levels were unexpected, as metabolic cross-feeding between acetate-producing bifidobacteria and acetate-consuming butyrate producers is known to occur (40, 46–50). Targeting of specific acetate and butyrate genes through gene prediction from 16S sequence data confirmed that acetate kinase was present at higher abundance in the *in vitro* system than butyrate kinase and acetyl-CoA transferase, and the same trend was observed in the XOS fermentations compared to that in the no-prebiotic controls (51). Low butyrate production could be attributed to the effects of pH, which were previously reported to influence bacterial communities and the production of SCFA *in vitro* (52, 53). This implies that improved buffering or pH control should be considered when designing batch *in vitro* models to study fecal communities and their metabolic by-products.

Prebiotics are defined, in part, by virtue of their utilization by host microbes (54). Although a functional demonstration of the specific mechanisms by which XOS transport and utilization occur in bifidobacteria has not yet been established, two models have been proposed (55–58). In one model, extracellular xylolytic enzymes degrade XOS, and then xylose monomers are transported into the cell (30). Alternatively, XOS are transported via an ABC transport system, and intracellular XOS is hydrolyzed (55, 56). The resulting xylose monomers are phosphorylated to form xylulose-5-P which then enters the *Bifidobacterium* shunt (55). Gene clusters encoding putative glycosyl hydrolases have been identified, including GH8, GH43, and GH120 (59–61). These clusters include genes encoding nonreducing end β-xylosidase, reducing end xylose-releasing exo-oligoxylanase, and endo-1,4-β-xylanase, each having a preferred oligomer length (59). Based on the current genome annotations, the presence of GH43 and GH120 clusters and genes encoding ABC-type permeases in *B. longum* subsp. *longum* CR15 suggests that the strain was capable of intracellular degradation of XOS.

Like other *in vitro* models, limitations exist with the IVE method (62). Additional improvements to be considered include pH control, minimization of the filtering of fecal slurries, and the use of different substrate concentrations to replicate more colon-like conditions. However, despite these limitations, the IVE model serves as a

useful tool to identify potential synergistic pairs and then for testing those pairings across multiple samples. Such *in vitro* methodologies can accelerate the process of strain discovery and synbiotic pairing prior to *in vivo* trials to validate these formulations. Finally, more sophisticated and controlled *in vitro* models would provide a basis for greater throughput and increase the library of strains that can be collected in a short amount of time.

Other attempts to identify synbiotic combinations have generally relied on pairing previously isolated probiotic strains with one or more prebiotics (63–66). Indeed, these and many of the other synbiotic combinations described in the literature would be considered complementary. While these approaches have the advantage of having characterized strains as the probiotic component, there is no *a priori* reason why the prebiotic would necessarily support growth of the probiotic *in vivo*. Accordingly, the enrichment method described in this study provides a basis for identifying putative probiotic strains that would be predicted to outcompete other resident microbes for the prebiotic. Provided these probiotic-prebiotic combinations result in a health benefit to the host, they would satisfy the definition of a synergistic synbiotic. Following this study, an appropriately designed multiple-arm synbiotic human clinical trial would be necessary to demonstrate synergistic effects and health benefits of the synbiotic combination described here.

MATERIALS AND METHODS

Sample collection. A total of 20 fecal samples were collected from volunteers throughout the duration of the study. Each participant was asked to sign a consent form indicating that the participant had no known gastrointestinal disease, was 19 years of age or older, had not consumed antibiotics or probiotic supplements in the last 6 months, was not a regular consumer of yogurt, and was willing to provide 1 to 3 stool samples over 3 months. Participants were given a commode specimen collection kit (Fisher Scientific, NH, USA) and detailed instructions for collection and preservation. The study was approved by the UNL Institutional Review Board (IRB 20160616139).

Samples were collected and processed in an anaerobic chamber (Bactron IV anaerobic chamber; Sheldon Manufacturing, Cornelius, OR, USA) (5% H_2, 5% CO_2, 90% N_2). Samples were diluted (1:10) in phosphate-buffered saline (PBS) at pH 7, homogenized, and stored in 2-ml aliquots at −80°C.

Stepwise fecal fermentations. For all enrichment and establishment experiments, XOS95, a 95% pure prebiotic substrate, was used (Prenexus Health, AZ, USA). For all fermentations, each fecal sample was treated as an individual experimental unit. In enrichment experiments, stepwise *in vitro* batch fermentations were performed. Diluted fecal slurries were homogenized, filtered, and mixed with fermentation broth (67) in a 6:3 ratio (vol/vol) in a total volume of 9.0 ml. When added, XOS was present at a concentration of 1%. All fermentations were incubated anaerobically at 37°C. After 24 h, 100-fold dilutions were performed by transferring 100 μl of sample to 9.9 ml of fermentation broth containing XOS. Three subsequent transfers were performed every 24 h, for a total of 96 h. Samples at 0, 24, 48, 72, and 96 h were collected and stored at −20°C for DNA extraction and SCFA analysis. At the end of the four fermentation cycles (96 h), samples were plated onto *Bifidobacterium* selective iodoacetate mupirocin (BSIM) and colonies were picked (68). Each colony isolated was grown in modified de Man, Rogosa and Sharpe (mMRS) from which glucose was omitted but which was supplemented with 1% XOS (mMRS-XOS). The isolates were stored at −20°C for subsequent DNA extraction, 16S Sanger sequencing, and identification.

For the establishment experiments, similar batchwise fermentations were conducted, except that the XOS-enriched strains obtained as described above were inoculated at the beginning of the fermentation cycle. Test strains were first incubated in MRS broth for 24 h and used to inoculate (1%) fresh fecal fermentation media, with or without 1% XOS. Subsequent transfers were carried out as before. Samples were collected every 24 h for up to 7 days, and isolates were picked from BSIM plates, grown in mMRS-XOS, and stored. Initial enrichment experiments were performed with 3 fecal samples, and 20 samples were used for subsequent establishment experiments with *B. longum* subsp. *longum* CR15.

DNA extraction and 16S Sanger sequencing and analysis. DNA from the samples collected (fermentation media and isolates) was extracted using phenol-chloroform as described by Martínez et al. (69), except that incubation times were for 30 min and DNA pellets were resuspended in 100 μl of DNase-free water. For the isolates, PCR was performed using 16S primers 8F (5′-AGAGTTTGATCCTGGC TCAG-3′) and 1391R (5′-GACGGGCGGTGTGTRCA-3′), and PCR products were purified using a QIAquick PCR purification kit (Qiagen, Hilden, Germany) and quantified with a NanoDrop ND-1000 spectrophotometer (Thermo Fisher, MA, USA). The purified PCR products were sequenced by the Genomics Core Facility at Michigan State University. Preliminary identification of potential IVE probiotic isolates was conducted using NCBI BLASTn. Species were assigned based on an identity threshold of ≥98.7% sequence similarity. The BLAST search revealed 3 different species represented by 7 strains that were each aligned to unique reference sequences.

Quantification of bifidobacteria using qPCR. For all *in vitro* fermentation experiments, quantification of bacterial groups in the fermentation samples was performed by quantitative PCR (qPCR) using a

TABLE 2 Primer sequences and PCR programs used to target different groups of *Bifidobacterium*

Target organism (reference)	Primer[a]		qPCR program
	Direction	Sequence (5′→3′)	
Bifidobacterium (79)	Forward	TCG CGT CYG GTG TGA AAG	Initial denaturation at 95°C for 5 min, 35 cycles at 95°C for 15 s, 58°C for 20 s, and 68°C for 30 s.
	Reverse	CCA CAT CCA GCR TCC AC	
B. pseudocatenulatum (80)	Forward	AGC CAT CGT CAA GGA GCT TAT CGC AG	Initial denaturation at 95°C for 5 min, 40 cycles at 94°C for 15 s, 68°C for 15 s, and 72°C for 15 s.
	Reverse	CAC GAC GTC CTG CTG AGA GCT CAC	
B. longum (81)	Forward	TTC CAG TTG ATC GCA TGG TCT TCT	Initial denaturation at 95°C for 10 min, 30 cycles at 95°C for 15 s, 65°C for 1 min, and 72°C for 45 s.
	Reverse	GGC TAC CCG TCG AAG CCA CG	
B. adolescentis (81)	Forward	GGA TCG GCT GGA GCT TGC TCC G	Initial denaturation at 95°C for 10 min, 30 cycles at 95°C for 15 s, 63°C for 1 min, and 72°C for 45 s.
	Reverse	CCC CGA AGG CTT GCT CCC AGT	
B. longum subsp. *longum* CR15 (this paper)	Forward	CCG CAT CAC AAC TGC TAT TGG	Initial denaturation at 95°C for 5 min, 30 cycles at 95°C for 15 s, 58°C for 15 s, and 72°C for 20 s.
	Reverse	CGA AAG CCC CAA TTT GTT CGT	

[a]Primers specific to the bifidobacterial species or strain of interest were used to track bacterial enrichment or establishment.

Mastercycler Realplex2 (Eppendorf AG, Hamburg, Germany). Each reaction mixture contained 12.5 μl of qPCR Master Mix (2× Maxima SYBR green; Thermo Fisher Scientific, MA, USA), 0.4 μM specific primers for each target organism (Table 2), 8.5 μl of water, and 3 μl of template DNA for a final volume of 25 μl. Duplicate wells were used for each sample. Samples that had a standard deviation of greater than 0.5 were reanalyzed. For each assay, standard curves were made using DNA isolated from pure cultures from which counts were determined through plate counting. A 10-fold serial dilution of the DNA standards was made, and the cycle threshold (C_T) values of the standards were plotted against $\log_{10}$ CFU/ml values.

Genome sequencing and assembly of *B. longum* subsp. *longum* CR15. For whole-genome sequencing, DNA extraction was performed using a QIAamp DNA Minikit (Qiagen, Hilden, Germany), and a genomic library was prepared using the Nextera XT DNA Library Prep kit. The genome of *B. longum* subsp. *longum* CR15 was sequenced on an Illumina MiSeq, resulting in 603,691 paired reads that were assembled *de novo* using the SPAdes Genome Assembler (ver 3.11) and aligned against a reference genome using Mauve (70, 71). A draft genome consisting of 63 contigs with 123-fold coverage was obtained postassembly.

Gene annotation was performed using PROKKA (72). Additionally, the draft genome was annotated against the CAZy database using dbCAN and the transportDB 2.0 database through TransAAP to identify carbohydrate active enzyme clusters and sugar transporters, respectively (73, 74).

Strain-specific primer design and validation. Rapid identification of PCR primers for unique core sequences (RUCS) was used to identify unique targets in the draft genome of *B. longum* subsp. *longum* CR15 and for *in silico* PCR (75). The unique target sequence was identified through alignment with complete genomes of 8 closely related *B. longum* subsp. *longum* strains that were retrieved from the NCBI database (see Table S1 in the supplemental material). Primer specificity was confirmed by a BLAST search against the NCBI RefSeq representative genome database for bacteria with NCBI Primer BLAST. Only 1 hit for a strain of *Gelidibacter algens*, a nonresident of the human gut, matched the primer pair. The adenine-specific methyltransferase PaeR71 gene was subsequently selected as the target amplicon with a length of 210 bp with the primer pair CCGCATCACAACTGCTATTGG (forward) and CGAAAGCCCCAAT TTGTTCGT (reverse) (Invitrogen, CA, USA). A gradient PCR was used to determine the suitable annealing temperature of 58°C. Experimental primer validation with both PCR and qPCR was performed using 11 strains in our culture collection that had a 95% to 100% identity at the 16S rRNA level (see Table S2).

Separation of XOS fractions and growth measurement. To obtain XOS fractions of specific degrees of polymerization (DPs), XOS was purified through exclusion chromatography using Biogel P-2 fine beads (Bio-Rad Laboratories, Hercules, CA). Fractions were collected and analyzed by thin-layer chromatography (TLC). Fractions were then pooled based on a DP of $\leq$4 and a DP of $>$4, lyophilized, and used for growth curves.

The ability of *B. longum* subsp *longum* CR15 to grow on XOS and its fractions was determined in mMRS containing 1% XOS, 1% XOS fraction containing DPs 2, 3, and 4, and 1% XOS fraction containing DPs of 4 and above. Controls were prepared in mMRS either with 1% glucose (mMRS-glucose) or with the equivalent amount of residual carbohydrates present in the 95% pure XOS (approximately 0.035%, final concentration [mMRS-res]). The residual sugars were predicted to be equal proportions of glucose, fructose, and sucrose based on the manufacturer's specification sheet. Furthermore, the mMRS medium was prepared at half strength (i.e., using only half the amount of ingredients present in standard MRS) in order to minimize growth on background carbohydrates.

The strain was first streaked onto MRS plates from frozen stock cultures and incubated for 48 h anaerobically at 37°C. Single colonies were isolated and inoculated in MRS broth for 24 h at 37°C. Then, 1% (vol/vol) of the cultures was transferred into fresh MRS. These subcultures were incubated for 12 h overnight before they were inoculated at 1% (vol/vol) into prewarmed prereduced mMRS, mMRS-glucose, mMRS-XOS, mMRS-DP2,3,4, mMRS-DP4, or mMRS-res in 200-μl volumes. Cultures were then incubated anaerobically at 37°C, and growth was determined by measuring the optical density at 600 nm

every 4 h for the first 12 h and again at 24 h in triplicates using a plate reader (Synergy HTX plate reader; BioTek, VT, USA).

16S rRNA amplicon sequencing and analysis. 16S rRNA amplicon sequencing was performed on DNA extracted from fecal fermentations. Samples were sequenced on a 2 × 250 bp MiSeq sequencer, using primers for the V4 region of the 16S sequence. A total of 4,397,582 sequences were obtained, with a mean of 36,954 sequences per sample.

Sequences were analyzed using QIIME2. Paired-end sequences were demultiplexed prior to importing into QIIME. FastQC was used to check sample sequence quality. Using the DADA2 workflow (https://benjjneb.github.io/dada2/), chimeric sequences were removed and forward and reverse reads were truncated to 240 bp and 200 bp, respectively (76). Sequences were dereplicated into unique amplicon sequence variants (ASV) with DADA2, and a list of exact representative sequences was created. ASV refers to the exact sequences that are resolved through the DADA2 pipeline, as described previously (76). The resulting product is an ASV table recording the number of times by which an ASV was observed in each sample. A total of 974 features were identified. Taxonomy was assigned using the Greengenes database with the pretrained classifier based on 99% sequence identity. Alpha diversity measures were calculated using a sample depth of 5171 sequences.

Statistical analysis for community sequencing data was done in QIIME and RStudio (ver 3.4.3). Two different alpha diversity measurements, Shannon index and observed ASVs, were computed. Pairwise comparisons between each treatment and time point were made using the Kruskal-Wallis test. FDR correction was incorporated for all statistical tests, and significance was determined using a significance cutoff at 0.05. For beta diversity, principal-coordinate analysis (PCoA) and principal-component analysis (PCA) plots were prepared to compare community compositions. The vegan (https://github.com/vegandevs/vegan) package was used to compute Bray-Curtis distance and conduct permutational multivariate analysis of variance (PERMANOVA). Comparisons of the relative abundances of specific ASVs between XOS treatments at 96 h were conducted using Wilcoxon rank sum test and visualized using Metacoder (77). Only taxa that had a relative abundance of greater than 0.1% were included in the analysis.

Short/branched-chain fatty acid analysis. S/BCFA concentrations were determined for all 20 fecal samples at all sample times using gas chromatography, similarly to Yang and Rose (67). Briefly, 0.4 ml of fermentation supernatant was vortexed with approximately 0.16 g of NaCl and 0.2 ml of 9 M sulfuric acid. Subsequently, 0.5 ml of diethyl ether was added, and tubes were shaken and briefly centrifuged. Then, 1 μl of the extract was injected into a gas chromatograph (Clarus 580; PerkinElmer, Waltham, MA, USA) with a fused silica capillary column (Nukol, 30 m by 0.25-mm inner diameter by 0.25-μm film thickness; Sigma-Aldrich, St. Louis, MO, USA). Quantification of S/BCFA was carried out as described previously (67). Six samples could not be quantified due to insufficient amounts of analyte. Subjects that comprised any of these samples were removed and S/BCFA concentrations for 14 of 20 subjects were used for the final statistical analysis. For comparison between treatments at every time point, a Kruskal-Wallis test was conducted along with Wilcoxon rank sum test with FDR adjustment.

PICRUSt (78) was used to relate taxonomic abundances from 16S data to functional S/BCFA metabolic genes, based on the Kyoto Encyclopedia of Genes and Genomes (KEGG) ontology database. Correlation analysis between taxa and S/BCFA was also performed using the 16S sequencing data and all available S/BCFA concentrations. In addition, mean relative abundances of taxa and S/BCFA predicted metabolic genes were visualized for each treatment.

Data availability. Whole-genome sequence of *B. longum* subsp. *longum* CR15 and 16S rRNA sequencing of fermentation samples were uploaded in the NCBI database and can be found under accession numbers PRJNA540282 and PRJNA540304, respectively.

SUPPLEMENTAL MATERIAL

Supplemental material for this article may be found at https://doi.org/10.1128/AEM.01073-19.

SUPPLEMENTAL FILE 1, PDF file, 0.3 MB.

ACKNOWLEDGMENTS

We thank Prenexus Health for providing us with XOS for all experiments and Yibo Xian, Qinnan Yang, and Mallory Van Haute for their assistance with DNA sequencing.

R.H. has received grants and honoraria from several food and ingredient companies, is a co-owner of Synbiotic Solutions, LLC, and is on the board of directors of the International Scientific Association for Probiotics and Prebiotics.

Amanda Li was supported by the NSF Research Experience for Undergraduates program.

REFERENCES

1. Simon J-C, Marchesi JR, Mougel C, Selosse M-A. 2019. Host-microbiota interactions: from holobiont theory to analysis. Microbiome 7:5. https://doi.org/10.1186/s40168-019-0619-4.
2. Rowland I, Gibson G, Heinken A, Scott K, Swann J, Thiele I, Tuohy K. 2018. Gut microbiota functions: metabolism of nutrients and other food components. Eur J Nutr 57:1–24. https://doi.org/10.1007/s00394-017-1445-8.

3. David LA, Maurice CF, Carmody RN, Gootenberg DB, Button JE, Wolfe BE, Ling AV, Devlin AS, Varma Y, Fischbach MA, Biddinger SB, Dutton RJ, Turnbaugh PJ. 2014. Diet rapidly and reproducibly alters the human gut microbiome. Nature 505:559–563. https://doi.org/10.1038/nature12820.
4. Makki K, Deehan EC, Walter J, Bäckhed F. 2018. The impact of dietary fiber on gut microbiota in host, health and disease. Cell Host Microbe 23:705–715. https://doi.org/10.1016/j.chom.2018.05.012.
5. Carding S, Verbeke K, Vipond DT, Corfe BM, Owen LJ. 2015. Dysbiosis of the gut microbiota in disease. Microb Ecol Heal Dis 26:26191. https://doi.org/10.3402/mehd.v26.26191.
6. Peterson CT, Sharma V, Elmén L, Peterson SN. 2015. Immune homeostasis, dysbiosis and therapeutic modulation of the gut microbiota. Clin Exp Immunol 179:363–377. https://doi.org/10.1111/cei.12474.
7. Sartor RB. 2008. Therapeutic correction of bacterial dysbiosis discovered by molecular techniques. Proc Natl Acad Sci U S A 105:16413–16414. https://doi.org/10.1073/pnas.0809363105.
8. Coen M, Want EJ, Clayton TA, Rhode CM, Young SH, Keun HC, Cantor GH, Metz AL, Robertson DG, Reily MD, Holmes E, Lindon JC, Nicholson JK. 2009. Mechanistic aspects and novel biomarkers of responder and non-responder phenotypes in galactosamine-induced hepatitis. J Proteome Res 8:5175–5187. https://doi.org/10.1021/pr9005266.
9. Healey GR, Murphy R, Brough L, Butts CA, Coad J. 2017. Interindividual variability in gut microbiota and host response to dietary interventions. Nutr Rev 75:1059–1080. https://doi.org/10.1093/nutrit/nux062.
10. Noecker C, Borenstein E. 2016. Getting personal about nutrition. Trends Mol Med 22:83–85. https://doi.org/10.1016/j.molmed.2015.12.010.
11. Zeevi D, Korem T, Zmora N, Israeli D, Rothschild D, Weinberger A, Ben-Yacov O, Lador D, Avnit-Sagi T, Lotan-Pompan M, Suez J, Mahdi JA, Matot E, Malka G, Kosower N, Rein M, Zilberman-Schapira G, Dohnalová L, Pevsner-Fischer M, Bikovsky R, Halpern Z, Elinav E, Segal E. 2015. Personalized nutrition by prediction of glycemic responses. Cell 163:1079–1094. https://doi.org/10.1016/j.cell.2015.11.001.
12. Krumbeck JA, Walter J, Hutkins RW. 2018. Synbiotics for improved human health: recent developments, challenges, and opportunities. Annu Rev Food Sci Technol 9:451–479. https://doi.org/10.1146/annurev-food-030117-012757.
13. Davis LMG, Martínez IS, Walter J, Goin C, Hutkins RW. 2011. Barcoded pyrosequencing reveals that consumption of galactooligosaccharides results in a highly specific bifidogenic response in humans. PLoS One 6:e25200. https://doi.org/10.1371/journal.pone.0025200.
14. Silk DBA, Davis A, Vulevic J, Tzortzis G, Gibson GR. 2009. Clinical trial: the effects of a *trans*-galactooligosaccharide prebiotic on faecal microbiota and symptoms in irritable bowel syndrome. Aliment Pharmacol Ther 29:508–518. https://doi.org/10.1111/j.1365-2036.2008.03911.x.
15. Vulevic J, Juric A, Walton GE, Claus SP, Tzortzis G, Toward RE, Gibson GR. 2015. Influence of galacto-oligosaccharide mixture (B-GOS) on gut microbiota, immune parameters and metabonomics in elderly persons. Br J Nutr 114:586–595. https://doi.org/10.1017/S0007114515001889.
16. Li T, Lu X, Yang X. 2017. Evaluation of clinical safety and beneficial effects of stachyose-enriched α-galacto-oligosaccharides on gut microbiota and bowel function in humans. Food Funct 8:262–269. https://doi.org/10.1039/c6fo01290f.
17. Gurry T, Gibbons SM, Nguyen LTT, Kearney SM, Ananthakrishnan A, Jiang X, Duvallet C, Kassam Z, Alm EJ. 2018. Predictability and persistence of prebiotic dietary supplementation in a healthy human cohort. Sci Rep 8:12699. https://doi.org/10.1038/s41598-018-30783-1.
18. Martínez I, Kim J, Duffy PR, Schlegel VL, Walter J. 2010. Resistant starches types 2 and 4 have differential effects on the composition of the fecal microbiota in human subjects. PLoS One 5:e15046. https://doi.org/10.1371/journal.pone.0015046.
19. Kok CR, Hutkins R. 2018. Yogurt and other fermented foods as sources of health-promoting bacteria. Nutr Rev 76:4–15. https://doi.org/10.1093/nutrit/nuy056.
20. Tilman D. 1977. Resource competition between plankton algae: an experimental and theoretical approach. Ecol Soc Am 58:338–348. https://doi.org/10.2307/1935608.
21. Hibbing ME, Fuqua C, Parsek MR, Peterson SB. 2010. Bacterial competition: surviving and thriving in the microbial jungle. Nat Rev Microbiol 8:15–25. https://doi.org/10.1038/nrmicro2259.
22. Bartosch S, Woodmansey EJ, Paterson JCM, McMurdo MET, Macfarlane GT. 2005. Microbiological effects of consuming a synbiotic containing *Bifidobacterium bifidum*, *Bifidobacterium lactis*, and oligofructose in elderly persons, determined by real-time polymerase chain reaction and counting of viable bacteria. Clin Infect Dis 40:28–37. https://doi.org/10.1086/426027.
23. Morelli L, Zonenschain D, Callegari ML, Grossi E, Maisano F, Fusillo M. 2003. Assessment of a new synbiotic preparation in healthy volunteers: survival, persistence of probiotic strains and its effect on the indigenous flora. Nutr J 2:11. https://doi.org/10.1186/1475-2891-2-11.
24. Kolida S, Gibson GR. 2011. Synbiotics in health and disease. Annu Rev Food Sci Technol 2:373–393. https://doi.org/10.1146/annurev-food-022510-133739.
25. Krumbeck JA, Maldonado-Gomez MX, Martínez I, Frese SA, Burkey TE, Rasineni K, Ramer-Tait AE, Harris EN, Hutkins RW, Walter J. 2015. *In vivo* selection to identify bacterial strains with enhanced ecological performance in synbiotic applications. Appl Environ Microbiol 81:2455–2465. https://doi.org/10.1128/AEM.03903-14.
26. Davis LMG, Martínez I, Walter J, Hutkins R. 2010. A dose dependent impact of prebiotic galactooligosaccharides on the intestinal microbiota of healthy adults. Int J Food Microbiol 144:285–292. https://doi.org/10.1016/j.ijfoodmicro.2010.10.007.
27. Arboleya S, Bottacini F, O'Connell-Motherway M, Ryan CA, Ross RP, Van Sinderen D, Stanton C. 2018. Gene-trait matching across the *Bifidobacterium longum* pan-genome reveals considerable diversity in carbohydrate catabolism among human infant strains. BMC Genomics 19:33. https://doi.org/10.1186/s12864-017-4388-9.
28. Wong CB, Sugahara H, Odamaki T, Xiao JZ. 2018. Different physiological properties of human-residential and non-human-residential bifidobacteria in human health. Benef Microbes 9:111–122. https://doi.org/10.3920/BM2017.0031.
29. Finegold SM, Li Z, Summanen PH, Downes J, Thames G, Corbett K, Dowd S, Krak M, Heber D. 2014. Xylooligosaccharide increases bifidobacteria but not lactobacilli in human gut microbiota. Food Funct 5:403–445. https://doi.org/10.1039/c3fo60348b.
30. Amaretti A, Bernardi T, Leonardi A, Raimondi S, Zanoni S, Rossi M. 2013. Fermentation of xylo-oligosaccharides by *Bifidobacterium adolescentis* DSMZ 18350: kinetics, metabolism, and β-xylosidase activities. Appl Microbiol Biotechnol 97:3109–3117. https://doi.org/10.1007/s00253-012-4509-y.
31. Rivière A, Selak M, Lantin D, Leroy F, De Vuyst L. 2016. Bifidobacteria and butyrate-producing colon bacteria: importance and strategies for their stimulation in the human gut. Front Microbiol 7:979. https://doi.org/10.3389/fmicb.2016.00979.
32. Aachary AA, Prapulla SG. 2011. Xylooligosaccharides (XOS) as an emerging prebiotic: microbial synthesis, utilization, structural characterization, bioactive properties, and applications. Compr Rev Food Sci Food Saf 10:2–16. https://doi.org/10.1111/j.1541-4337.2010.00135.x.
33. Marotti I, Bregola V, Aloisio I, Di Gioia D, Bosi S, Di Silvestro R, Quinn R, Dinelli G. 2012. Prebiotic effect of soluble fibres from modern and old durum-type wheat varieties on *Lactobacillus* and *Bifidobacterium* strains. J Sci Food Agric 92:2133–2140. https://doi.org/10.1002/jsfa.5597.
34. Kiran Kondepudi K, Ambalam P, Nilsson I, Wadström T, Ljungh Å. 2012. Prebiotic-non-digestible oligosaccharides preference of probiotic bifidobacteria and antimicrobial activity against *Clostridium difficile*. Anaerobe 18:489–497. https://doi.org/10.1016/j.anaerobe.2012.08.005.
35. Maldonado-Gómez MX, Martínez I, Bottacini F, O'Callaghan A, Ventura M, van Sinderen D, Hillmann B, Vangay P, Knights D, Hutkins RW, Walter J. 2016. Stable engraftment of *Bifidobacterium longum* AH1206 in the human gut depends on individualized features of the resident microbiome. Cell Host Microbe 20:515–526. https://doi.org/10.1016/j.chom.2016.09.001.
36. Fujiwara S, Seto Y, Kimura A, Hashiba H. 2001. Intestinal transit of an orally administered streptomycin-rifampicin-resistant variant of *Bifidobacterium longum* SBT2928: its long-term survival and effect on the intestinal microflora and metabolism. J Appl Microbiol 90:43–52. https://doi.org/10.1046/j.1365-2672.2001.01205.x.
37. Walter J, Maldonado-Gómez MX, Martínez I. 2018. To engraft or not to engraft: an ecological framework for gut microbiome modulation with live microbes. Curr Opin Biotechnol 49:129–139. https://doi.org/10.1016/j.copbio.2017.08.008.
38. Reid G, Gaudier E, Guarner F, Huffnagle GB, Macklaim JM, Munoz AM, Martini M, Ringel-Kulka T, Sartor BR, Unal RR, Verbeke K, Walter J, International Scientific Association for Probiotics and Prebiotics. 2010. Responders and non-responders to probiotic interventions: how can we improve the odds? Gut Microbes 1:200–204. https://doi.org/10.4161/gmic.1.3.12013.
39. Cummings JH, Macfarlane GT. 1997. Role of intestinal bacteria in nutrient

metabolism. Clin Nutr 16:3–11. https://doi.org/10.1016/S0261-5614(97)80252-X.
40. Brahma S, Martínez I, Walter J, Clarke J, Gonzalez T, Menon R, Rose DJ. 2017. Impact of dietary pattern of the fecal donor on *in vitro* fermentation properties of whole grains and brans. J Funct Foods 29:281–289. https://doi.org/10.1016/j.jff.2016.12.042.
41. Chen T, Long W, Zhang C, Liu S, Zhao L, Hamaker BR. 2017. Fiber-utilizing capacity varies in *Prevotella*- versus *Bacteroides*-dominated gut microbiota. Sci Rep 7:2594. https://doi.org/10.1038/s41598-017-02995-4.
42. Ntemiri A, Ní Chonchuír F, O'Callaghan TF, Stanton C, Ross RP, O'Toole PW. 2017. Glycomacropeptide sustains microbiota diversity and promotes specific taxa in an artificial colon model of elderly gut microbiota. J Agric Food Chem 65:1836–1846. https://doi.org/10.1021/acs.jafc.6b05434.
43. Koutsos A, Lima M, Conterno L, Gasperotti M, Bianchi M, Fava F, Vrhovsek U, Lovegrove JA, Tuohy KM. 2017. Effects of commercial apple varieties on human gut microbiota composition and metabolic output using an *in vitro* colonic model. Nutrients 9:E533. https://doi.org/10.3390/nu9060533.
44. Flint HJ, Duncan SH, Scott KP, Louis P. 2015. Links between diet, gut microbiota composition and gut metabolism. Proc Nutr Soc 74:13–22. https://doi.org/10.1017/S0029665114001463.
45. Morrison DJ, Preston T. 2016. Formation of short chain fatty acids by the gut microbiota and their impact on human metabolism. Gut Microbes 7:189–200. https://doi.org/10.1080/19490976.2015.1134082.
46. Belenguer A, Duncan SH, Calder AG, Holtrop G, Louis P, Lobley GE, Flint HJ. 2006. Two routes of metabolic cross-feeding between *Bifidobacterium adolescentis* and butyrate-producing anaerobes from the human gut. Appl Environ Microbiol 72:3593–3599. https://doi.org/10.1128/AEM.72.5.3593-3599.2006.
47. Rios-Covian D, Gueimonde M, Duncan SH, Flint HJ, de los Reyes-Gavilan CG. 2015. Enhanced butyrate formation by cross-feeding between *Faecalibacterium prausnitzii* and *Bifidobacterium adolescentis*. FEMS Microbiol Lett 362:fnv176. https://doi.org/10.1093/femsle/fnv176.
48. den Besten G, Lange K, Havinga R, van Dijk TH, Gerding A, van Eunen K, Müller M, Groen AK, Hooiveld GJ, Bakker BM, Reijngoud D-J. 2013. Gut-derived short-chain fatty acids are vividly assimilated into host carbohydrates and lipids. Am J Physiol Gastrointest Liver Physiol 305:G900–G910. https://doi.org/10.1152/ajpgi.00265.2013.
49. Gargari G, Taverniti V, Balzaretti S, Ferrario C, Gardana C, Simonetti P, Guglielmetti S. 2016. Consumption of a *Bifidobacterium bifidum* strain for 4 weeks modulates dominant intestinal bacterial taxa and fecal butyrate in healthy adults. Appl Environ Microbiol 82:5850–5859. https://doi.org/10.1128/AEM.01753-16.
50. Rivière A, Gagnon M, Weckx S, Roy D, De Vuyst L. 2015. Mutual cross-feeding interactions between *Bifidobacterium longum* subsp. *longum* NCC2705 and *Eubacterium rectale* ATCC 33656 explain the bifidogenic and butyrogenic effects of arabinoxylan oligosaccharides. Appl Environ Microbiol 81:7767–7781. https://doi.org/10.1128/AEM.02089-15.
51. Duncan SH, Barcenilla A, Stewart CS, Pryde SE, Flint HJ. 2002. Acetate utilization and butyryl coenzyme A (CoA):acetate-CoA transferase in butyrate-producing bacteria from the human large intestine. Appl Environ Microbiol 68:5186–5190. https://doi.org/10.1128/aem.68.10.5186-5190.2002.
52. Walker AW, Duncan SH, Carol E, Leitch M, Child MW, Flint HJ. 2005. pH and peptide supply can radically alter bacterial populations and short-chain fatty acid ratios within microbial communities from the human colon. Appl Environ Microbiol 71:3692–3700. https://doi.org/10.1128/AEM.71.7.3692-3700.2005.
53. Belenguer A, Duncan SH, Holtrop G, Anderson SE, Lobley GE, Flint HJ. 2007. Impact of pH on lactate formation and utilization by human fecal microbial communities. Appl Environ Microbiol 73:6526–6533. https://doi.org/10.1128/AEM.00508-07.
54. Gibson GR, Hutkins R, Sanders ME, Prescott SL, Reimer RA, Salminen SJ, Scott K, Stanton C, Swanson KS, Cani PD, Verbeke K, Reid G. 2017. Expert consensus document: the International Scientific Association for Probiotics and Prebiotics (ISAPP) consensus statement on the definition and scope of prebiotics. Nat Rev Gastroenterol Hepatol 14:491–502. https://doi.org/10.1038/nrgastro.2017.75.
55. Gilad O, Jacobsen S, Stuer-Lauridsen B, Pedersen MB, Garrigues C, Svensson B. 2010. Combined transcriptome and proteome analysis of *Bifidobacterium animalis* subsp. *lactis* BB-12 grown on xylo-oligosaccharides and a model of their utilization. Appl Environ Microbiol 76:7285–7291. https://doi.org/10.1128/AEM.00738-10.
56. Palframan RJ, Gibson GR, Rastall RA. 2003. Carbohydrate preferences of *Bifidobacterium* species isolated from the human gut. Curr Issues Intest Microbiol 4:71–75.
57. Gullón P, Moura P, Esteves MP, Girio FM, Domínguez H, Parajó JC. 2008. Assessment on the fermentability of xylooligosaccharides from rice husks by probiotic bacteria. J Agric Food Chem 56:7482–7487. https://doi.org/10.1021/jf800715b.
58. van den Broek LAM, Hinz SWA, Beldman G, Vincken JP, Voragen A. 2008. *Bifidobacterium* carbohydrases-their role in breakdown and synthesis of (potential) prebiotics. Mol Nutr Food Res 52:146–163. https://doi.org/10.1002/mnfr.200700121.
59. Lagaert S, Pollet A, Delcour JA, Lavigne R, Courtin CM, Volckaert G. 2011. Characterization of two β-xylosidases from *Bifidobacterium adolescentis* and their contribution to the hydrolysis of prebiotic xylooligosaccharides. Appl Microbiol Biotechnol 92:1179–1185. https://doi.org/10.1007/s00253-011-3396-y.
60. Lagaert S, Van Campenhout S, Pollet A, Bourgois TM, Delcour JA, Courtin CM, Volckaert G. 2007. Recombinant expression and characterization of a reducing-end xylose-releasing exo-oligoxylanase from *Bifidobacterium adolescentis*. Appl Environ Microbiol 73:5374–5377. https://doi.org/10.1128/AEM.00722-07.
61. Cecchini DA, Laville E, Laguerre S, Robe P, Leclerc M, Doré J, Henrissat B, Remaud-Siméon M, Monsan P, Potocki-Véronèse G. 2013. Functional metagenomics reveals novel pathways of prebiotic breakdown by human gut bacteria. PLoS One 8:e72766. https://doi.org/10.1371/journal.pone.0072766.
62. Pham VT, Mohajeri MH. 2018. The application of in vitro human intestinal models on the screening and development of pre- and probiotic. Benef Microbes 9:725–742. https://doi.org/10.3920/BM2017.0164.
63. Adamberg S, Sumeri I, Uusna R, Ambalam P, Kondepudi KK, Adamberg K, Wadström T, Ljungh Å. 2014. Survival and synergistic growth of mixed cultures of bifidobacteria and lactobacilli combined with prebiotic oligosaccharides in a gastrointestinal tract simulator. Microb Ecol Health Dis 25:23062. https://doi.org/10.3402/mehd.v25.23062.
64. Bielecka M, Biedrzycka E, Majkowska A. 2002. Selection of probiotics and prebiotics for synbiotics and confirmation of their *in vivo* effectiveness. Food Res Int 35:125–131. https://doi.org/10.1016/S0963-9969(01)00173-9.
65. Grimoud J, Durand H, De Souza S, Monsan P, Ouarné F, Theodorou V, Roques C. 2010. *In vitro* screening of probiotics and synbiotics according to anti-inflammatory and anti-proliferative effects. Int J Food Microbiol 144:42–50. https://doi.org/10.1016/j.ijfoodmicro.2010.09.007.
66. Mazzola G, Aloisio I, Biavati B, Di Gioia D. 2015. Development of a synbiotic product for newborns and infants. Lebenson Wiss Technol 64:727–734. https://doi.org/10.1016/j.lwt.2015.06.033.
67. Yang J, Rose DJ. 2014. Long-term dietary pattern of fecal donor correlates with butyrate production and markers of protein fermentation during in vitro fecal fermentation. Nutr Res 34:749–759. https://doi.org/10.1016/j.nutres.2014.08.006.
68. Lewis ZT, Totten SM, Smilowitz JT, Popovic M, Parker E, Lemay DG, Van Tassell ML, Miller MJ, Jin Y-S, German JB, Lebrilla CB, Mills DA. 2015. Maternal fucosyltransferase 2 status affects the gut bifidobacterial communities of breastfed infants. Microbiome 3:13. https://doi.org/10.1186/s40168-015-0071-z.
69. Martínez I, Stegen JC, Maldonado-Gómez MX, Eren AM, Siba PM, Greenhill AR, Walter J. 2015. The gut microbiota of rural Papua New Guineans: composition, diversity patterns, and ecological processes. Cell Rep 11:527–538. https://doi.org/10.1016/j.celrep.2015.03.049.
70. Darling ACE, Mau B, Blattner FR, Perna NT. 2004. Mauve: multiple alignment of conserved genomic sequence with rearrangements. Genome Res 14:1394–1403. https://doi.org/10.1101/gr.2289704.
71. Bankevich A, Nurk S, Antipov D, Gurevich AA, Dvorkin M, Kulikov AS, Lesin VM, Nikolenko SI, Pham S, Prjibelski AD, Pyshkin AV, Sirotkin AV, Vyahhi N, Tesler G, Alekseyev MA, Pevzner PA. 2012. SPAdes: a new genome assembly algorithm and its applications to single-cell sequencing. J Comput Biol 19:455–477. https://doi.org/10.1089/cmb.2012.0021.
72. Seemann T. 2014. Prokka: rapid prokaryotic genome annotation. Bioinformatics 30:2068–2069. https://doi.org/10.1093/bioinformatics/btu153.
73. Huang L, Zhang H, Wu P, Entwistle S, Li X, Yohe T, Yi H, Yang Z, Yin Y. 2018. dbCAN-seq: a database of carbohydrate-active enzyme (CAZyme) sequence and annotation. Nucleic Acids Res 46:D516–D521. https://doi.org/10.1093/nar/gkx894.
74. Elbourne LDH, Tetu SG, Hassan KA, Paulsen IT. 2017. TransportDB 2.0: a

database for exploring membrane transporters in sequenced genomes from all domains of life. Nucleic Acids Res 45:D320–D324. https://doi.org/10.1093/nar/gkw1068.
75. Christen M, Thomsen F, Hasman H, Westh H, Lya Kaya H, Lund O. 2017. RUCS: rapid identification of PCR primers for unique core sequences. Bioinformatics 33:3917–3921. https://doi.org/10.1093/bioinformatics/btx526.
76. Callahan BJ, McMurdie PJ, Rosen MJ, Han AW, Johnson AJA, Holmes SP. 2016. DADA2: high-resolution sample inference from Illumina amplicon data. Nat Methods 13:581–583. https://doi.org/10.1038/nmeth.3869.
77. Foster ZSL, Sharpton TJ, Grünwald NJ, Lefort M, Malumbres OJ, Vink C. 2017. Metacoder: an R package for visualization and manipulation of community taxonomic diversity data. PLoS Comput Biol 13:e1005404. https://doi.org/10.1371/journal.pcbi.1005404.
78. Langille MGI, Zaneveld J, Caporaso JG, McDonald D, Knights D, Reyes JA, Clemente JC, Burkepile DE, Vega Thurber RL, Knight R, Beiko RG, Huttenhower C. 2013. Predictive functional profiling of microbial communities using 16S rRNA marker gene sequences. Nat Biotechnol 31:814–821. https://doi.org/10.1038/nbt.2676.
79. Martínez I, Wallace G, Zhang C, Legge R, Benson AK, Carr TP, Moriyama EN, Walter J. 2009. Diet-induced metabolic improvements in a hamster model of hypercholesterolemia are strongly linked to alterations of the gut microbiota. Appl Environ Microbiol 75:4175–4184. https://doi.org/10.1128/AEM.00380-09.
80. Junick J, Blaut M. 2012. Quantification of human fecal *Bifidobacterium* species by use of quantitative real-time PCR analysis targeting the *groEL* gene. Appl Environ Microbiol 78:2613–2622. https://doi.org/10.1128/AEM.07749-11.
81. Rinne MM, Gueimonde M, Kalliomäki M, Hoppu U, Salminen SJ, Isolauri E. 2005. Similar bifidogenic effects of prebiotic-supplemented partially hydrolyzed infant formula and breastfeeding on infant gut microbiota. FEMS Immunol Med Microbiol 43:59–65. https://doi.org/10.1016/j.femsim.2004.07.005.

Bifidobacteria strains primer design	**NCBI accession no.**
Bifidobacterium longum subsp*. longum* KACC 91563, complete genome	CP002794.1
Bifidobacterium longum subsp*. longum* strain AH1206, complete genome	CP016019.1
Bifidobacterium longum subsp*. longum* JCM 1217 DNA, complete genome	AP010888.1
Bifidobacterium longum subsp. longum strain NCIMB809, complete genome	CP011964.1
Bifidobacterium longum subsp*. longum* GT15, complete genome	CP006741.1
Bifidobacterium longum subsp*. longum* BBMN68, complete genome	CP002286.1
Bifidobacterium longum subsp*. longum* strain CCUG30698, complete genome	CP011965.1
Bifidobacterium longum subsp*. longum* JDM301, complete genome	CP002010.1

Table S1. *Bifidobacterium* genomes used for *B. longum* subsp *longum* CR15 primer design. Whole genome sequences from closely related strains were used to identify unique target sequences in *B. longum* subsp *longum* CR15. The adenine-specific methyltransferase PaeR71 gene was selected as the target amplicon for *B. longum* subsp *longum* CR15.

Bifidobacteria strains for primer validation	% identity at 16S rRNA gene level
B. longum subsp*. longum* AH120	100%
B. longum subsp*. longum* (ATCC® 15707™)	99%
B. longum longum F8	100%
B. longum longum JDM301	99%
B. longum DJO10A	100%
Bifidobacterium sp. 12_1_47BFAA	100%
Bifidobacterium sp. 113	95%
Bifidobacterium sp. HMLN14	96%
B. adolescentis ATCC 15703	95%
B. adolescentis L2-32	95%
B. adolescentis IVS-1	96%

Table S2. *Bifidobacterium* strains used for primer validation. *Bifidobacterium* strains that shared a 95-100% identity at the 16S rRNA gene level were used to validate the specificity of the *B. longum* subsp *longum* CR15 primer. Only DNA extracted from *B. longum* subsp *longum* CR15 displayed amplification with the primer.

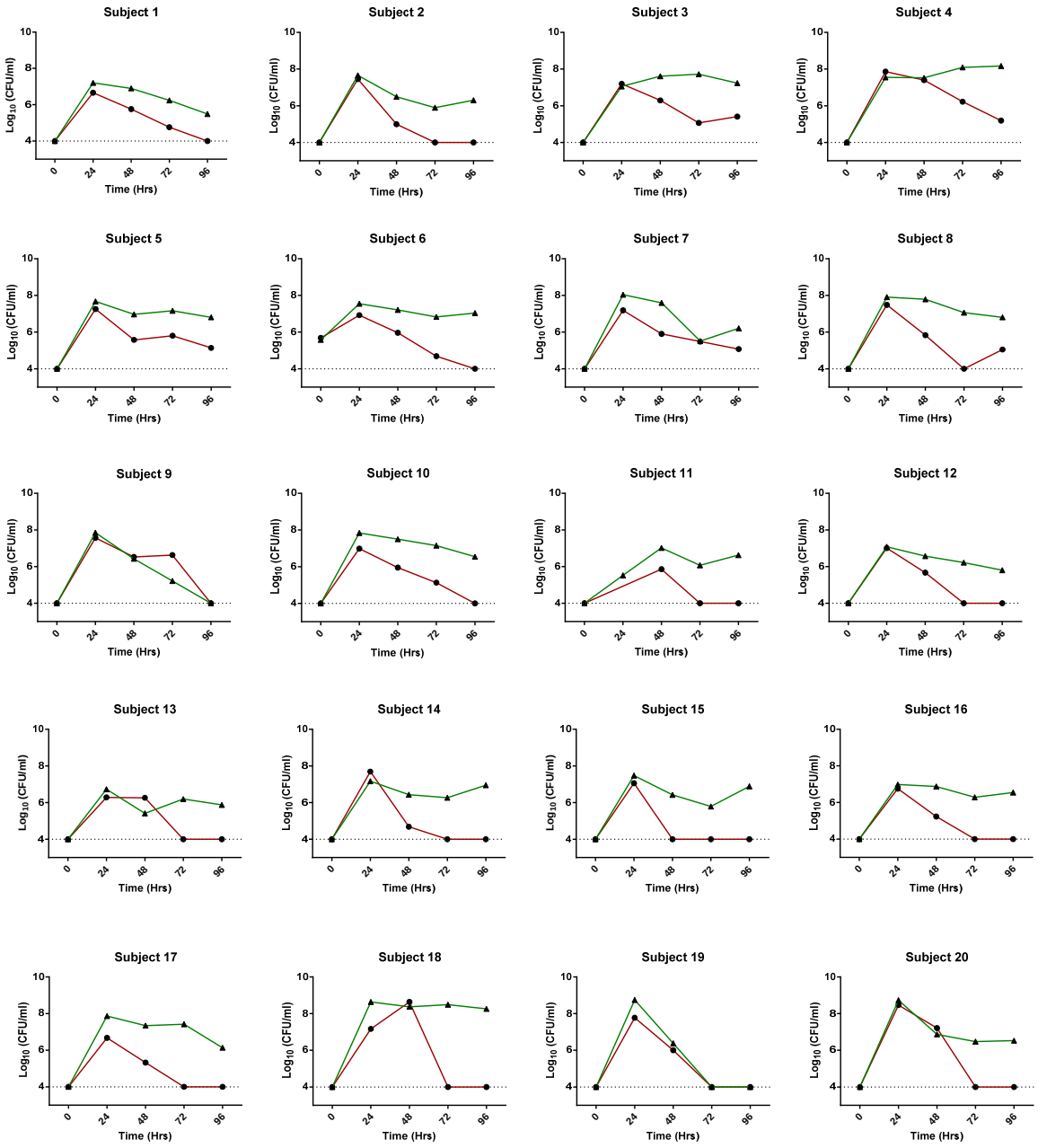

FIG S1. Establishment of *B. longum* subsp. *longum* CR15 after inoculation into 20 individual fecal samples in the presence (▲) or absence (●) of XOS. For each experiment, the strain was inoculated at 10^7 CFU/mL and quantified by RT-qPCR using strain-specific primers. *B. longum* subsp *longum* CR15 was initially isolated from Subject 6. Horizontal dashed lines indicate the limit of detection (10^4 CFU/mL).

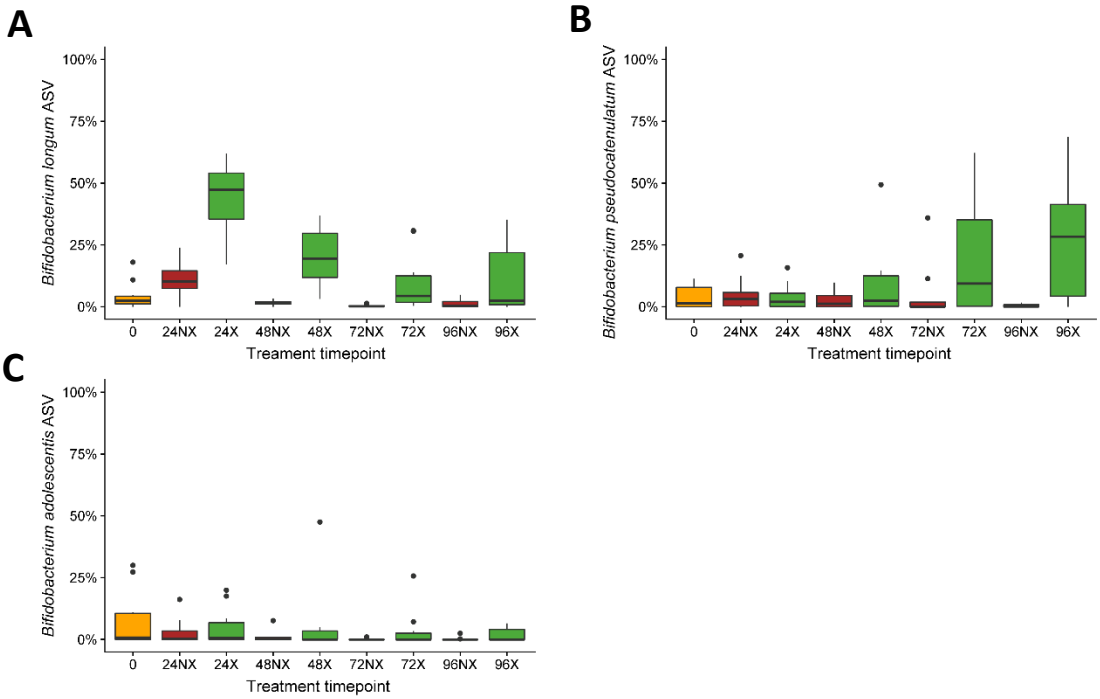

FIG S2. Relative abundances of specific species of bifidobacteria in establishment experiments. Abundance of ASVs corresponding to *B. longum* **(A)**, *B. pseudocatenulatum* (**B)** and *B. adolescentis* (**C)** in the presence of XOS displayed as relative abundance at each time point. 0; baseline of samples at the start of fermentation; NX, fermentation without XOS; X, fermentations with XOS.

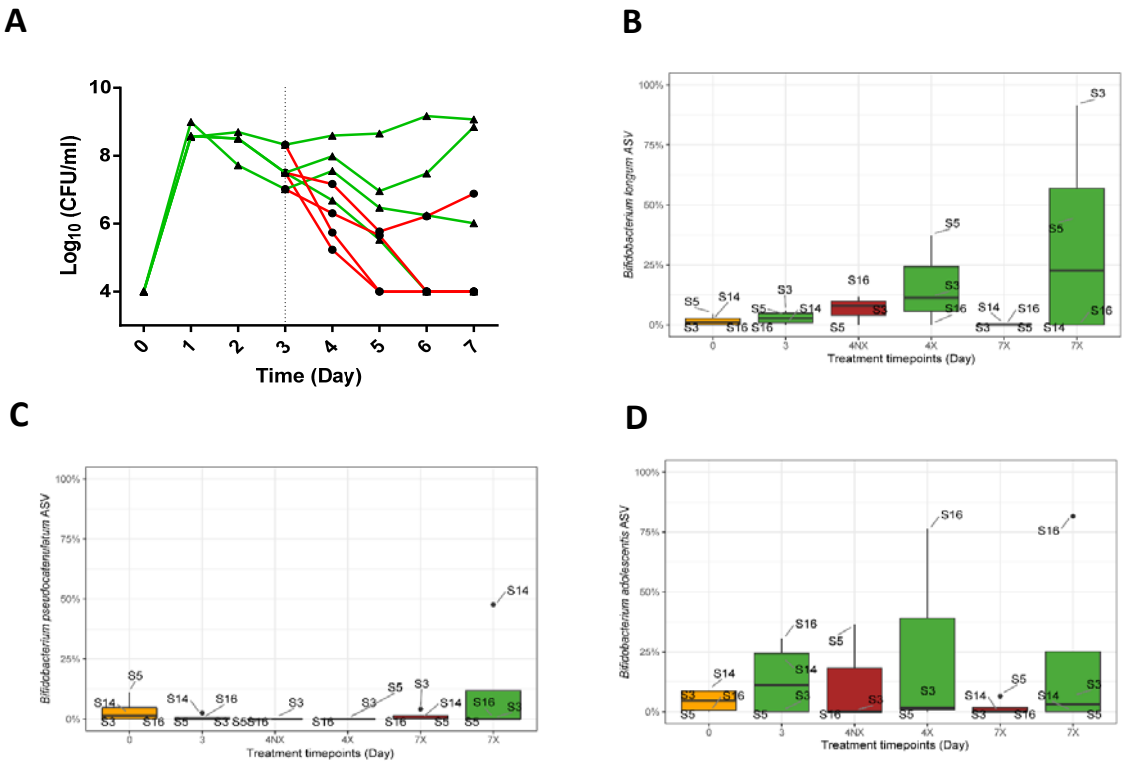

Fig S3. 7-day fermentation experiment further demonstrates dependency of B. longum subsp longum CR15 on XOS along with host-dependent response. Samples were first supplemented with XOS and step-wise transfers were carried out for the first 3 days. A split was done during day 3 with parallel transfers into XOS-containing fermenters and in fermenters without XOS. Subsequent step-wise transfers were conducted from day 4 to day 7 following the respective treatments at the split. 16S sequencing was carried out for samples for Days 0, 3, 4 7. **A)** qPCR quantification of *B. longum* subsp *longum* CR15 throughout fermentation with (▲) and without (•) XOS in the 4 samples tested **B-D)** Relative abundance of specific Amplicon Sequence Variants (ASVs) corresponding to *B. longum*, *B. pseudocatenulatum* and *B. adolescentis* throughout fermentation. 0 (yellow), baseline of samples at the start of fermentation; NX (red), fermentation without XOS; X (green), fermentations with XOS. Day 4 samples for S14 were not sequenced.

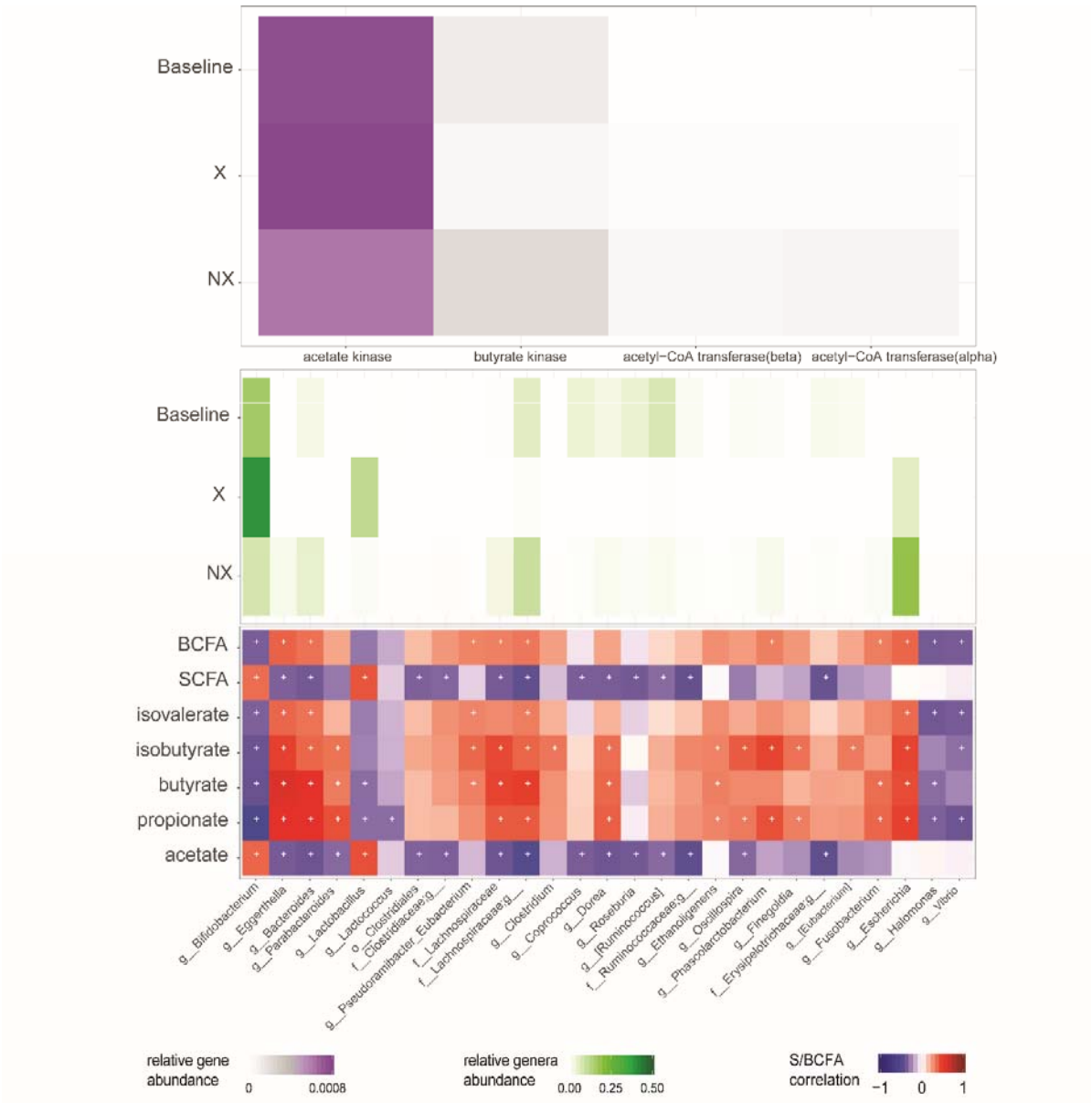

FIG S4. Mean relative abundances for taxa and predicted S/BCFA genes and correlation of microbial fermentation metabolites with genera identified in the fermentation samples. Only genera that had at least one significant correlation with a metabolite were mapped. + significant correlation between genus abundance and concentration of metabolite (FDR<0.05). SCFA; short chain fatty acids, BCFA; branched chain fatty acids, X; XOS, NX; No XOS.